Palmitic acid-induced autophagy increases reactive oxygen species via the Ca^{2+}/PKCα/NOX4 pathway and impairs endothelial function in human umbilical vein endothelial cells

PAN CHEN[1,2], HENGDAO LIU[2], HONG XIANG[1], JIANDA ZHOU[3], ZHENGPENG ZENG[4], RUIFANG CHEN[1], SHAOLI ZHAO[2], JIE XIAO[2], ZHIHAO SHU[2], SHUHUA CHEN[1,5] and HONGWEI LU[1,2]

[1]Center for Experimental Medical Research; Departments of [2]Cardiology, [3]Burns and [4]Respiratory Medicine, The Third Xiangya Hospital of Central South University; [5]Department of Biochemistry, School of Life Sciences of Central South University, Changsha, Hunan 410013, P.R. China

Received February 1, 2018; Accepted September 6, 2018

DOI: 10.3892/etm.2019.7269

Abstract. It is well known that the lipotoxic mechanism of palmitic acid (PA), a main constituent of triglyceride, is dependent on reactive oxygen species (ROS). Recently, it has also been reported that PA is an autophagy inducer. However, the causal association and underlying mechanism of induced autophagy and ROS in PA toxicity remain unclear. The present study demonstrates for the first time that PA-induced autophagy enhances ROS generation via activating the calcium ion/protein kinase Cα/nicotinamide adenine dinucleotide phosphate oxidase 4 (Ca^{2+}/PKCα/NOX4) pathway in human umbilical vein endothelial cells (HUVECs). It was revealed that PA treatment resulted in a significant increase in ROS generation and autophagic activity, leading to endothelial dysfunction as indicated by downregulated nitric oxide synthesis, decreased capillary-like structure formation and damaged cell repair capability. Furthermore, PA effectively activated the Ca^{2+}/PKCα/NOX4 pathway, which is indicative of upregulated cytosolic Ca^{2+} levels, activated PKCα and increased NOX4 protein expression. 3-Methyladenine was then used to inhibit autophagy, which significantly reduced PA-induced ROS generation and blocked the Ca^{2+}/PKCα/NOX4 pathway. The endothelial dysfunction caused by PA was ameliorated by downregulating ROS generation using a NOX4 inhibitor. In conclusion, PA-induced autophagy contributes to endothelial dysfunction by increasing oxidative stress via the Ca^{2+}/PKCα/NOX4 pathway in HUVECs.

Correspondence to: Dr Hongwei Lu, Center for Experimental Medical Research, The Third Xiangya Hospital of Central South University, 138 Tongzipo Road, Changsha, Hunan 410013, P.R. China
E-mail: hwlv2226@163.com

Dr Shuhua Chen, Department of Biochemistry, School of Life Sciences of Central South University, 172 Tongzipo Road, Changsha, Hunan 410013, P.R. China
E-mail: shuhuachen2013@163.com

Key words: palmitic acid, lipotoxicy, autophagy, reactive oxygen species, Endothelial cell dysfunction

Introduction

It has previously been reported that elevated triglyceride levels are a major risk factor for residual cardiovascular diseases (CVDs) (1). Hypertriglyceridemia is a common issue worldwide (2), and great attention has been given to identifying an appropriate treatment. Palmitic acid (PA), a major component of triglyceride in the blood (3), has been reported to induce cell dysfunction and death, particularly in nonadipose tissue cells, including pancreatic β cells, cardiomyocytes and hepatocytes (4). The lipotoxic effect of PA has been implicated in the pathogenesis of numerous CVDs (5). In addition, endothelial cells are important cellular components of the cardiovascular system, and therefore endothelial dysfunction is usually one of the early signs of CVD (6).

It is generally accepted that PA-induced cell death can occur due to increased reactive oxygen species (ROS) generation. A study recently reported that PA also serves an important role in the initiation of autophagy (7). ROS and autophagy have been linked to a number of pathophysiological mechanisms, and ROS at physiological concentrations are known to regulate redox homeostasis and kinase-driven signaling pathways (8). However, excessive ROS accumulation leads to oxidative stress that contributes to various malignancies and disorders (9). Macroautophagy, commonly known as autophagy, typically serves as a cell survival mechanism, although it can result in type II programmed cell death under certain conditions (10). Intracellular ROS are primarily generated as by-products in mitochondria (11). Certain enzymes, including nicotinamide adenine dinucleotide phosphate oxidases (NOXs), xanthine oxidase, endoplasmic reticulum oxidoreductase 1 and myeloperoxidase, as well as a number of organelles, including peroxisomes, are important sources of ROS generation (12,13). As reported previously, excess ROS generation enhances autophagic activity via multiple pathways, which in turn degrades impaired mitochondria to restore normal ROS levels (14). However, exorbitant autophagy results in lysosomal dysfunction and endoplasmic

reticulum stress (15). Although autophagy inhibition decreases ROS levels, the mechanism underlying this phenomenon remains to be elucidated (16).

The aim of the present study was to investigate the causal association between autophagy activation and ROS generation following PA treatment, as well as the molecular mechanism responsible for this effect in endothelial cells. The results revealed that PA-induced lipotoxicity is associated with autophagy activation, which enhances ROS generation via activating the calcium ion/protein kinase Cα/nicotinamide adenine dinucleotide phosphate oxidase 4 (Ca^{2+}/PKCα/NOX4) pathway in endothelial cells. These results provide an insight into the potential of treating CVD by targeting autophagy.

Materials and methods

Cell culture. Human umbilical vein endothelial cells (HUVECs) at passage 20 and 25 were used in all experiments (ATCC, Manassas, VA, USA). Cells were grown in Dulbecco's modified Eagle's medium (DMEM; Hyclone; GE Healthcare, Logan, UT, USA) supplemented with 10% fetal bovine serum (FBS; Hyclone; GE Healthcare) and 1% penicillin and streptomycin at 37˚C in an atmosphere containing 5% CO_2.

PA treatment. A solution of 10% (w/v) bovine serum albumin (BSA; Sigma-Aldrich; Merck KGaA, Darmstadt, Germany) was used to dissolve PA (Sigma-Aldrich; Merck KGaA) in order to obtain a final concentration of 0.3 mM. The autophagy inhibitor 3-methyladenine (3-MA; Selleck Chemicals, Houston, TX, USA) was dissolved in 0.3 mM PA at 1 M (PA+3-MA group) and NOX4 inhibitor GKT137831 (Selleck Chemicals) was dissolved in PA at 20 μM (PA+NOX4 inhibitor group). BSA (10%) alone was used as the vehicle control. All groups were treated at room temperature for 24 h.

Cell viability assessment. Cell viability was assessed using Cell Counting Kit-8 (CCK-8; Dojindo Molecular Technologies, Inc., Kumamoto, Japan). Briefly, cells were seeded at density of $1x10^4$ cells/well in 96-well plates. Cells were washed twice with PBS, following which CCK-8 reagent pre-mixed with DMEM at a ratio of 1:10 was added. Following incubation for 1 h, cell viability was measured by reading the absorbance at 450 nm on a microplate reader (EnVision XCite; PerkinElmer, Inc., Waltham, MA, USA).

ROS assay. Intracellular ROS production was measured using a 2',7'-dichlorodihydrofluorescein diacetate (DCFH-DA) assay according to the manufacturer's protocol (Beyotime Institute of Biotechnology, Haimen, China). Cells were washed thrice with serum-free DMEM, seeded in 6-well plates at a density of $2x10^5$ cells/well and incubated for 30 min at 37˚C with 1 ml DCFH-DA (1:1,000). Subsequently, cells were washed thrice with serum-free DMEM and observed under an inverted fluorescence microscope (Olympus Corp., Tokyo, Japan).

Cytosolic Ca2+ measurement. Fura-2 acetoxymethyl (AM; Beyotime Institute of Biotechnology) was used to measure the cytosolic Ca^{2+} concentration. Briefly, cells were seeded in 96-well plates at a density of $1x10^4$ cells/well and seeded with 2 μM Fura-2 AM diluted in Dulbecco's phosphate-buffered saline (DPBS). After incubation of 30 min, extracellular Fura-2 AM was then washed away three times by DPBS. Cellular fluorescence intensity measured at excitation wavelength of 340 and 380 nm. Cytosolic Ca^{2+} was expressed as the ratio of emitted fluorescence at 340 and 380 nm.

Cell repair capability measurement. A scratch-wound healing assay was performed to assess the repair ability of endothelial cells. Briefly, cells were seeded in 6-well plates at a density of $2x10^5$ cells/well marked with three equidistant parallel lines on the bottom of each well and starved for 24 h before the experiment. Subsequently, scratch wound was performed by a 10-μl max-volume pipette, the detached cells were washed away by DPBS. Three fields were selected for observation and imaging under a microscope (Olympus Corp.) when PA was added, images were taken and evaluated as 0 h. After PA treatment for 24 h, the same fields were assessed and marked as 24 h to evaluate the repair ability of endothelial cells.

Nitric oxide (NO) assay. NO generation in HUVECs was measured using a Nitrate/Nitrite Assay kit (Beyotime Institute of Biotechnology). Initially, cells were treated with PA for 24 h in 6-well plates. Supernatants were collected after centrifugation for 5 min at 500 x g at room temperature for the NO assay (Beyotime Institute of Biotechnology). Nitrate/Nitrite Assay reagents was added into these supernatants according to the manufacturer's protocol. NO expression was estimated by measuring the absorbance at 540 nm.

Matrigel tube formation assay. The formation of capillary-like structures by HUVECs was assessed using the Matrigel Basement Membrane Matrix (Corning Inc., Corning, NY, USA). Briefly, HUVECs were seeded in Matrigel-coated 96-well plates at a density of $5x10^4$ cells/cm^2. Tube formation was observed under an inverted phase fluorescent microscope (Olympus Corp.), and images were captured with a digital camera. The results were quantified by measuring the total length of the tubules in each well.

Western blotting. Total protein was extracted from the cells using radioimmunoprecipitation assay buffer (Beyotime Institute of Biotechnology) and quantified by BCA (Beyotime Institute of Biotechnology). Equal amounts of cellular proteins (20 μg) were separated by SDS-PAGE on 10% gel and transferred to a polyvinylidene membrane. After blocking with 5% non-fat milk at room temperature for 2 h, the membranes were incubated overnight at 4˚C with primary antibodies diluted at 1:1,000. The following primary antibodies were used: Light chain 3 (LC3; cat. no. 12741; Cell Signaling Technology, Inc., Danvers, MA, USA), PKCα (cat. no. sc-8393; Santa Cruz Biotechnology, Inc., Dallas, TX, USA), p-PKCα (cat. no. sc-377565; Santa Cruz Biotechnology, Inc.), p62 (cat. no. sc-28359; Santa Cruz Biotechnology, Inc.), NOX4 (cat. no. ab133303; Abcam, Cambridge, UK) and GAPDH (diluted at 1:2,000; cat. no. sc-47724; Santa Cruz Biotechnology, Inc.). BeyoECL Plus (cat. no. P0018; Beyotime Institute of Biotechnology) was used and the detected bands were quantified by densitometric analysis and normalized to those of the corresponding loading control GAPDH using ImageJ software k 1.45 (National Institutes of Health, Bethesda, MD, USA).

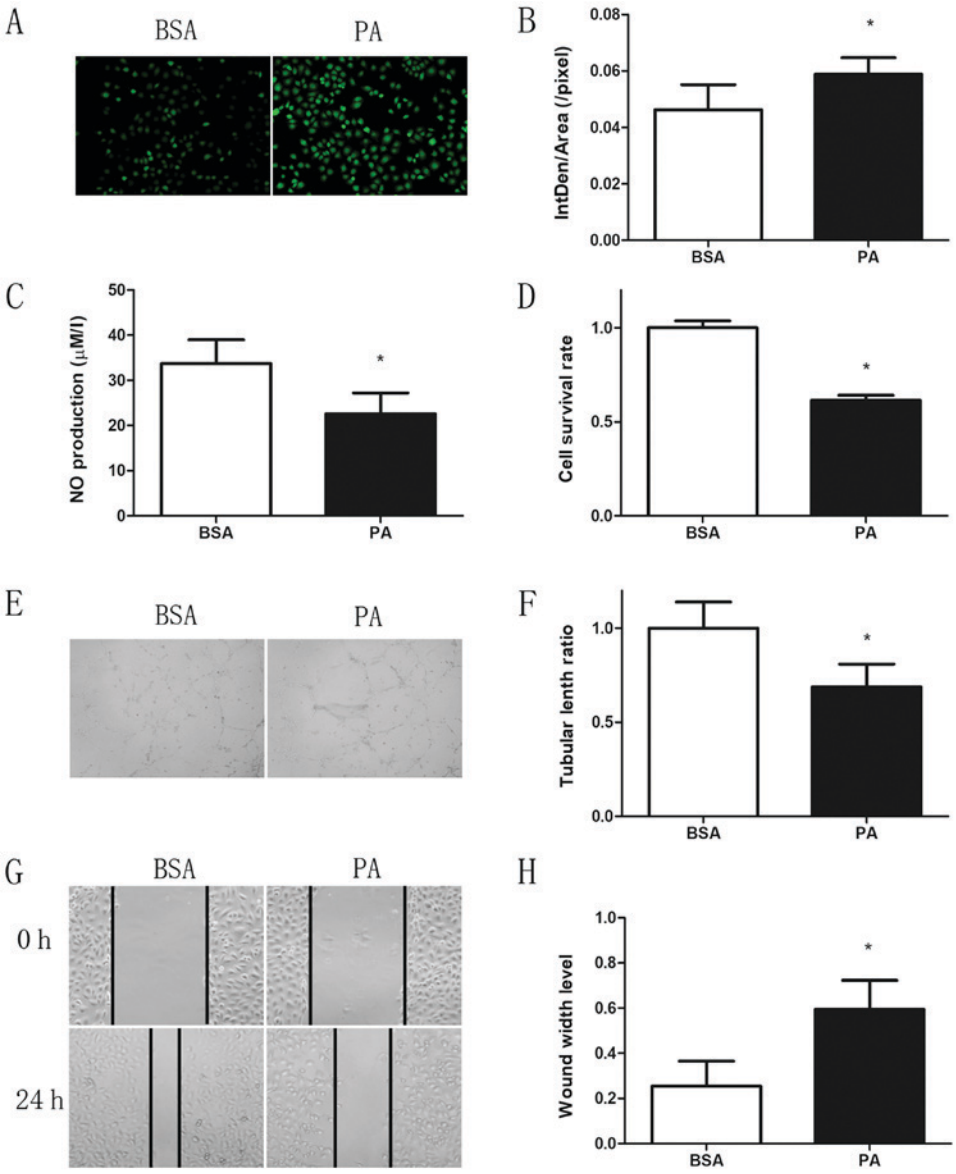

Figure 1. PA induces endothelial dysfunction in human umbilical vein endothelial cells (magnification, x400). Cells were treated with 10% BSA as a vehicle control or 0.3 mM PA for 24 h. (A) Representative fluorescence microscopy imaging and (B) quantitative analysis of reactive oxygen species generation. (C) Quantitative analysis of NO generation as assessed using a Nitrate/Nitrite assay kit. (D) Quantitative analysis of cell viability as assessed using a Cell Counting Kit-8 assay. (E) Representative imaging and (F) quantitative analysis of the capillary-like structure formation. (G) Representative wound healing assay images and (H) quantitative analysis of the repair ability of cells. Data are presented as the mean ± standard error of the mean of three independent experiments. *P<0.05 vs. vehicle control. PA, palmitic acid; BSA, bovine serum albumin; NO, nitric oxide.

Transmission electron microscopy. Cells were harvested following 24 h of treatment, washed with 0.1 M cacodylate buffer (cat. no. 37238-25, Nacalai Tesque, Inc., Kyoto, Japan), fixed in 1% agarose in 0.1 M cacodylate buffer and then post-fixed in 1% osmium tetroxide (cat. no. 75632; Sigma-Aldrich; Merck KGaA) for 2 h. Following dehydration in serially diluted ethanol solutions, the cells were embedded in an epoxy resin. Ultrathin (60-80 nm) sections were cut and placed on the slides. The sections on the slides were then double stained with uranyl acetate and lead nitrate prior to examining under a transmission electron microscope (HT-7700; Hitachi, Ltd., Tokyo, Japan).

Statistical analysis. Data were analyzed using IBM SPSS software (version 20.0; IBM Corp., Armonk, NY, USA) and are expressed as the mean ± standard error of the mean. Comparisons between multiple groups were assessed by Student-Newman-Keuls test, and P<0.05 was considered to indicate a statistically significant difference.

Results

PA induces endothelial dysfunction in HUVECs. To assess whether ROS generation and the subsequent decrease in NO synthesis serve a critical role in the pathogenesis of endothelial dysfunction, ROS and NO production was assessed in HUVECs treated with 0.3 mM PA for 24 h. As expected, treatment with PA for 24 h resulted in a significant increase in ROS generation and decrease in NO synthesis as compared with those observed in the control group (Fig. 1A-C). Cell viability was significantly

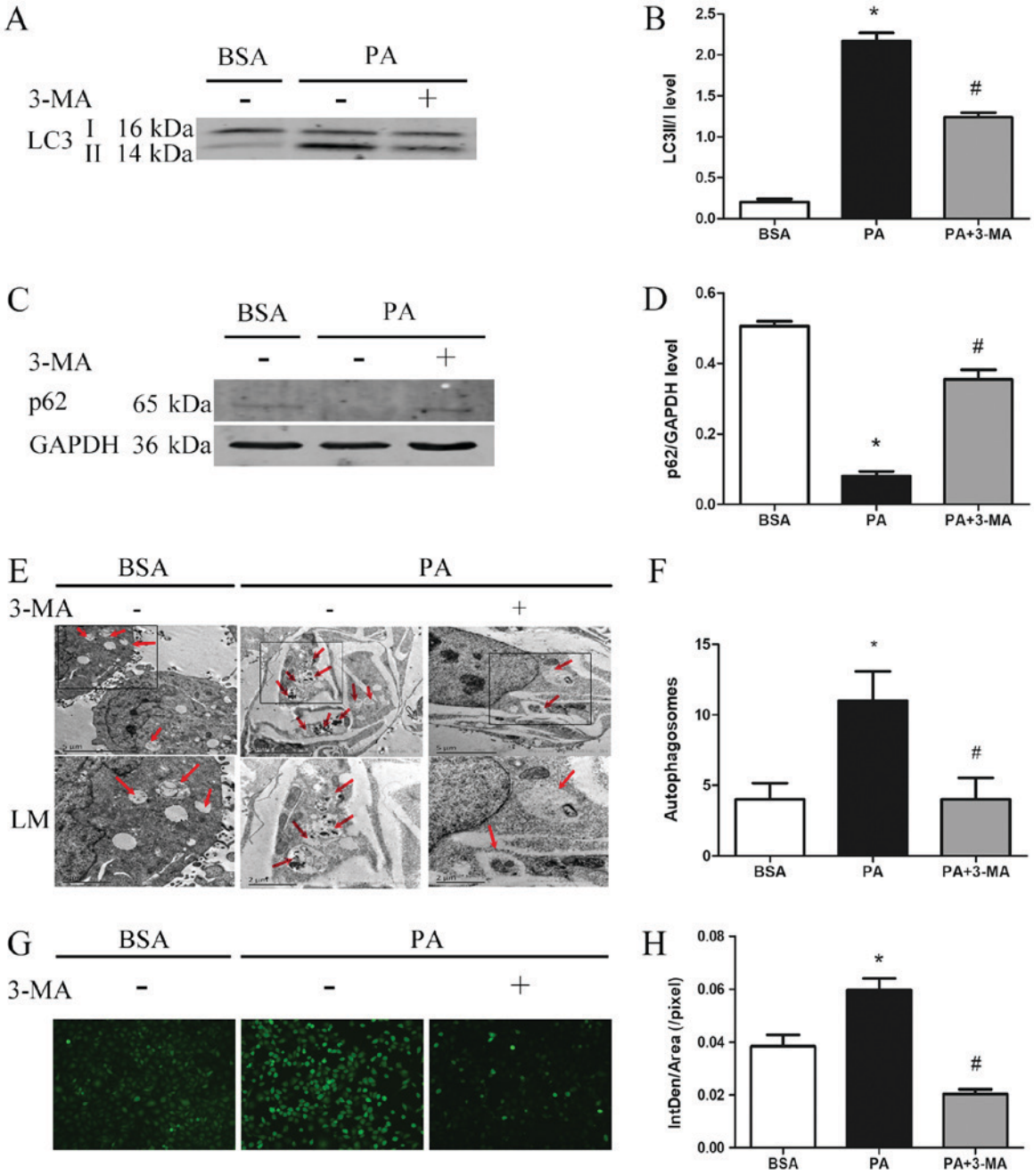

Figure 2. Inhibiting autophagy decreases PA-induced ROS accumulation. Human umbilical vein endothelial cells were treated with 0.3 mM PA alone or PA + 1 mM 3-MA for 24 h. BSA was used as the vehicle control. (A) Representative western blot images and (B) quantitative analysis of LC3 expression. (C) Representative western blot images and (D) quantitative analysis of p62 expression. (E) Representative electron microscope images and (F) quantitative analysis of autophagosomes in cells following treatment (arrows indicate autophagosomes). (G) Representative fluorescence assay images and (H) quantitative analysis of intracellular ROS generation. Data are presented as the mean ± standard error of the mean of three independent experiments. *P<0.05 vs. vehicle control; $^{\#}$P<0.05 vs. PA. PA, palmitic acid; ROS, reactive oxygen species; 3-MA, 3-methyladenine; BSA, bovine serum albumin; LC3, light chain 3; LM, local magnification.

decreased following PA treatment for 24 h, with ~60% of cells surviving (Fig. 1D). In addition, the ability to form capillary-like structures, which is a crucial indicator of angiogenesis, was markedly reduced following PA treatment (Fig. 1E and F). The repair ability of cells was also significantly suppressed by PA treatment, as observed by the reduced wound healing compared with the control group (Fig. 1G and H).

Autophagy inhibition decreases PA-induced ROS accumulation. To assess the effect of autophagy on ROS production, the autophagic activity was estimated by monitoring LC3 turnover and p62 degradation. The results were in agreement with previous observations (17). PA treatment was observed to significantly increase the LC3II/LC3I ratio (Fig. 2A and B), markedly decrease p62 expression (Fig. 2C and D) and significantly increase the number of autophagosomes (Fig. 2E and F). However, these effects of PA were blocked by 3-MA, a specific autophagy inhibitor (Fig. 2A-F). Furthermore, PA-induced ROS generation was significantly inhibited by 3-MA, suggesting that PA-induced ROS generation is autophagy-dependent (Fig. 2G and H).

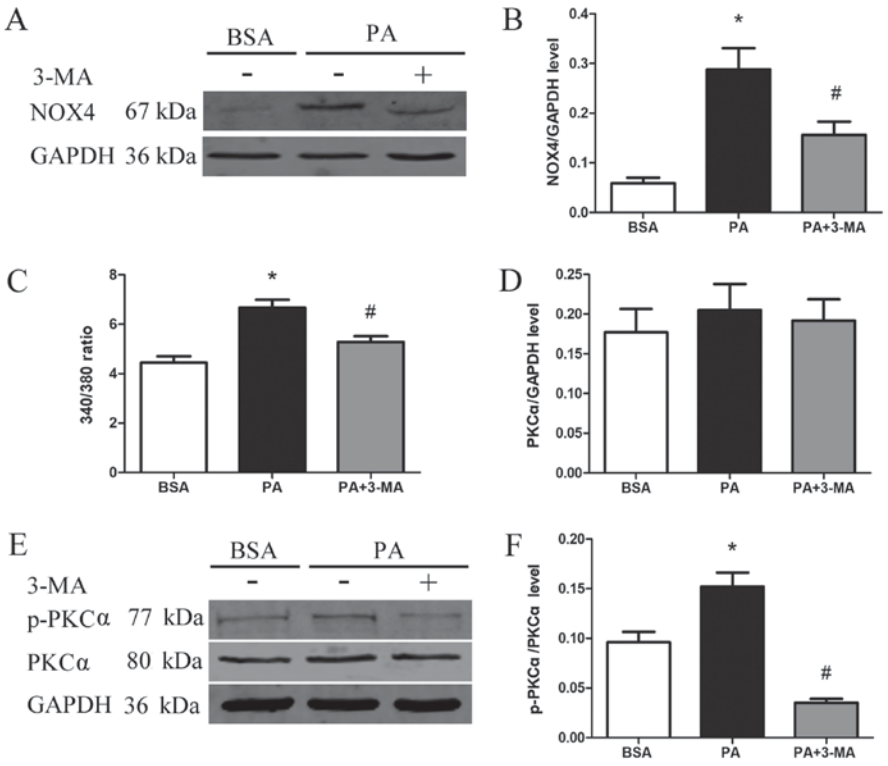

Figure 3. PA-induced autophagy activates the Ca^{2+}/PKCα/NOX4 pathway. Human umbilical vein endothelial cells were treated with 0.3 mM PA alone or PA + 1 mM 3-MA for 24 h. BSA was used as a vehicle control. (A) NOX4 protein expression was measured using western blotting, and (B) quantitative analysis of protein levels is shown. (C) Cytosolic Ca^{2+} levels were measured using Fura-2 AM, and the ratios of fluorescence intensity of Fura-2 AM at 340/380 nm were calculated. (D) Quantitative analysis and (E) representative western blots of PKCα expression. (F) Quantitative analysis of PKCα phosphorylate ratio. Data are presented as the mean ± standard error of the mean of three independent experiments. *P<0.05 vs. vehicle control; $^{\#}$P<0.05 vs. PA. PA, palmitic acid; 3-MA, 3-methyladenine; Ca^{2+}/PKCα/NOX4, calcium ion/protein kinase Cα/nicotinamide adenine dinucleotide phosphate oxidase 4; BSA, bovine serum albumin; AM, acetoxymethyl.

PA-induced autophagy activates the Ca^{2+}/PKCα/NOX4 pathway. NOX4 is an important source of intracellular ROS (18); therefore, the effect of PA-induced autophagy on NOX4 protein expression was assessed in the current study. NOX4 expression was significantly upregulated following PA treatment; however, treatment with the autophagy inhibitor 3-MA markedly blocked the PA-induced expression of NOX4 (Fig. 3A and B). In order to explore the mechanism responsible for PA-induced NOX4 expression, the cytosolic Ca^{2+} concentration and PKCα expression were assessed using Fura-2 AM and western blotting analyses, respectively. The results revealed that cytosolic Ca^{2+} content was significantly increased in PA-treated cells compared with that in control cells, while 3-MA evidently reduced cytosolic Ca^{2+} (Fig. 3C). Similarly, PKCα activation was upregulated following PA treatment, whereas it was significantly inhibited when 3-MA was also present in the culture medium (Fig. 3D-F). These results suggest that PA-induced autophagy was able to activate the Ca^{2+}/PKCα/NOX4 pathway.

NOX4 inhibition improves PA-induced HUVEC dysfunction. To determine the role of PA-mediated activation of the Ca^{2+}/PKCα/NOX4 pathway in endothelial dysfunction, the specific NOX4 inhibitor GKT137831 was used. The results revealed that GKT137831 significantly reduced PA-induced ROS generation (Fig. 4A and B). Furthermore, NOX4 inhibition reversed the PA-induced decrease in NO synthesis, as indicated by the increased intracellular NO levels (Fig. 4C). The PA-mediated damage in the formation of capillary-like structures was also alleviated by NOX4 inhibition (Fig. 4D and E). Finally, the repair ability of cells was significantly improved, as indicated by a narrower scratch wound at 24 h in cells treated with a combination of PA and GKT137831, as compared with those treated with PA alone (Fig. 4F and G). These results suggest that the PA-induced endothelial dysfunction is mediated through autophagy-dependent activation of the Ca^{2+}/PKCα/NOX4 pathway.

Discussion

In the present study a novel mechanism of PA-induced endothelial dysfunction in HUVECs was identified. Autophagy inhibition was demonstrated to downregulate PA-induced ROS generation by interfering with the Ca^{2+}/PKCα/NOX4 pathway. Alleviating ROS and oxidative stress affects numerous signaling pathways associated with cell survival, proliferation, vasodilation (NO generation) and angiogenesis (19-23).

A number of studies have linked autophagic activity to ROS generation (24-26). Generally, ROS activates autophagy, which inhibits excessive ROS generation in a negative feedback manner. ROS accumulation promotes autophagic activity via multiple mechanisms, including activation of adenosine 5'-monophosphate-activated protein kinase (27), promotion of high mobility group box 1 translocation from the nucleus to

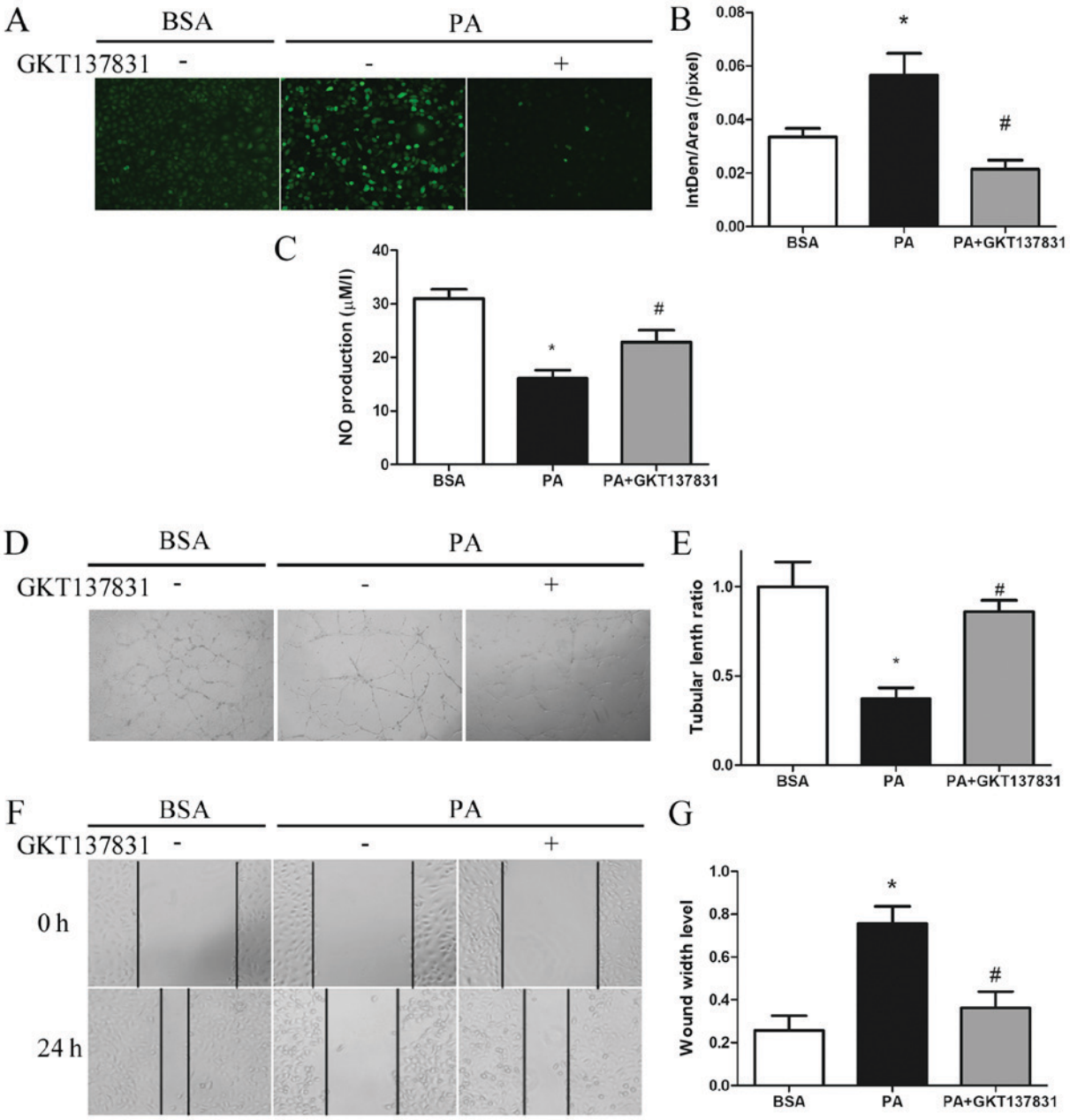

Figure 4. NOX4 inhibition ameliorated PA-induced HUVEC dysfunction (magnification, x400). HUVECs were treated with 0.3 mM PA in the presence or absence of 20 μM GKT137831. BSA was used as a vehicle control. (A) Reactive oxygen species production was measured by assessing the cell fluorescence in a given area, and (B) quantitative analysis of the results is shown. (C) NO production was measured using a commercial Nitrate/Nitrite assay kit. (D) Representative imaging and (E) quantitative analysis of the capillary-like structure formation of cells. (F) Representative wound healing images and (G) quantitative analysis of the repair ability of cells. Data are presented as the mean ± standard error of the mean of three independent experiments. *P<0.05 vs. vehicle control; #P<0.05 vs. PA. NOX4, nicotinamide adenine dinucleotide phosphate oxidase 4; PA, palmitic acid; HUVEC, human umbilical vein endothelial cell; BSA, bovine serum albumin; NO, nitric oxide.

the cytoplasm (28,29), and stabilization of hypoxia-inducible factor-1α (30,31). ROS-induced activation of autophagy clears damaged mitochondria and subsequently decreases ROS generation (24). Conversely, it has been reported that autophagy promotes ROS generation rather than suppressing it (16). In the present study, PA-induced ROS generation was significantly decreased when cells were simultaneously treated with an inhibitor, suggesting that autophagy possibly regulates ROS production. Based on these findings, the mechanism by which autophagy may promote ROS production was further explored, and it was demonstrated that 3-MA treatment reduced PA-induced cytosolic Ca^{2+} upregulation. Given that elevated cytosolic Ca^{2+} concentrations have been reported to activate NOXs via PKC activation (32), PKCα activation and NOX4 expression were examined in cells treated with PA and/or 3-MA. The results revealed that the inhibition of autophagy significantly decreased the PA-induced expression levels of p-PKCα and NOX4. Although NOX4 has been reported to activate phosphoinositide 3-kinase (33), 3-MA still effectively inhibited autophagy in HUVECs, as illustrated by the western blotting and electron microscopy results in the current study. In addition, using the specific NOX4 inhibitor GKT137831, it was confirmed that NOX4 suppression improved PA-induced endothelial dysfunction. Taken together, these findings suggest

that PA-induced ROS generation is achieved by activation autophagy via the Ca^{2+}/PKCα/NOX4 pathway.

In conclusion, the results of the present study suggested that PA-induced autophagy activates the Ca^{2+}/PKCα/NOX4 pathway to promote ROS generation. The novel pathway identified in the present study may help to improve our understanding of PA lipotoxicity, therefore providing a novel strategy that may have potential as a treatment for CVDs caused by hypertriglyceridemia.

Acknowledgements

The authors would like to thank Dr Wei Chen for guiding Matrigel tube formation assay and Dr Hui Peng for guiding the NO assay (both Center for Experimental Medical Research, The Third Xiangya Hospital of Central South University, Changsha, China).

Funding

The present study was supported by funding from the National Natural Science Foundation of China (grant nos. 8187035 2 and 81470593), the National Basic Research Program of China (grant no. 2014CB542400) and the Key Research and Development Project of Hunan Province (grant no. 2017SK2024).

Availability of data and materials

The datasets used and/or analyzed during the current study are available from the corresponding author on reasonable request.

Authors' contributions

All authors made substantial contributions to this research. Experiments were primarily performed by PC and HLiu, and were in charge of article editing and revision of the study. HX, ZZ, and SZ assisted in performing the experiment. Data were analyzed by JX, ZS and RC. JZ ensured that all questions related to accuracy and integrity of any part of the work are appropriately investigated and resolved. HLu and SC made substantial contributions to the conception and design of this research. HLu approved final version to be published.

Ethics approval and consent to participate

Not applicable.

Patient consent for publication

Not applicable.

Competing interests

The authors declare that they have no competing interests.

References

1. Fruchart JC, Sacks FM, Hermans MP, Assmann G, Brown WV, Ceska R, Chapman MJ, Dodson PM, Fioretto P, Ginsberg HN, *et al*: The residual risk reduction initiative: A call to action to reduce residual vascular risk in dyslipidaemic patient. Diab Vasc Dis Res 5: 319-335, 2008.
2. Miller M, Stone NJ, Ballantyne C, Bittner V, Criqui MH, Ginsberg HN, Goldberg AC, Howard WJ, Jacobson MS, Kris-Etherton PM, *et al*: Triglycerides and cardiovascular disease: A scientific statement from the American Heart Association. Circulation 123: 2292-2333, 2011.
3. Borradaile NM and Schaffer JE: Lipotoxicity in the heart. Curr Hypertens Rep 7: 412-417, 2005.
4. Brookheart RT, Michel CI and Schaffer JE: As a matter of fat. Cell Metab 10: 9-12, 2009.
5. Titov VN: The excess of palmitic fatty acid in food as main cause of lipoidosis of insulin-dependent cells: Skeletal myocytes, cardio-myocytes, periportal hepatocytes, kupffer macrophages and b-cells of pancreas. Klin Lab Diagn 61: 68-77, 2016 (In Russian).
6. Sena CM, Pereira AM and Seiça R: Endothelial dysfunction-a major mediator of diabetic vascular disease. Biochim Biophys Acta 1832: 2216-2231, 2013.
7. Khan MJ, Rizwan Alam M, Waldeck-Weiermair M, Karsten F, Groschner L, Riederer M, Hallström S, Rockenfeller P, Konya V, Heinemann A, *et al*: Inhibition of autophagy rescues palmitic acid-induced necroptosis of endothelial cells. J Biol Chem 287: 21110-21120, 2012.
8. Gough DR and Cotter TG: Hydrogen peroxide: A Jekyll and Hyde signalling molecule. Cell Death Dis 2: e213, 2011.
9. Schieber M and Chandel NS: ROS function in redox signaling and oxidative stress. Curr Biol 24: R453-R462, 2014.
10. Mariño G, Niso-Santano M, Baehrecke EH and Kroemer G: Self-consumption: The interplay of autophagy and apoptosis. Nat Rev Mol Cell Biol 15: 81-94, 2014.
11. Huang S, Van Aken O, Schwarzländer M, Belt K and Millar AH: The roles of mitochondrial reactive oxygen species in cellular signaling and stress response in plants. Plant Physiol 171: 1551-1559, 2016.
12. Arnhold J and Flemmig J: Human myeloperoxidase in innate and acquired immunity. Arch Biochem Biophys 500: 92-106, 2010.
13. Fransen M, Nordgren M, Wang B and Apanasets O: Role of peroxisomes in ROS/RNS-metabolism: Implications for human disease. Biochim Biophys Acta 1822: 1363-1373, 2012.
14. Scherz-Shouval R and Elazar Z: Regulation of autophagy by ROS: Physiology and pathology. Trends Biochem Sci 36: 30-38, 2011.
15. Almaguel FG, Liu JW, Pacheco FJ, De Leon D, Casiano CA and De Leon M: Lipotoxicity mediated cell dysfunction and death involves lysosomal membrane permeabilization and cathepsin L activity. Brain Res 1318: 133-143, 2010.
16. Gong J, Muñoz AR, Chan D, Ghosh R and Kumar AP: STAT3 down regulates LC3 to inhibit autophagy and pancreatic cancer cell growth. Oncotarget 5: 2529-2541, 2014.
17. Klionsky DJ, Abdalla FC, Abeliovich H, Abraham RT, Acevedo-Arozena A, Adeli K, Agholme L, Agnello M, Agostinis P, Aguirre-Ghiso JA, *et al*: Guidelines for the use and interpretation of assays for monitoring autophagy. Autophagy 8: 445-544, 2012.
18. Evangelista AM, Thompson MD, Bolotina VM, Tong X and Cohen RA: Nox4- and Nox2-dependent oxidant production is required for VEGF-induced SERCA cysteine-674 S-glutathiolation and endothelial cell migration. Free Radic Biol Med 53: 2327-2334, 2012.
19. Song P and Zou MH: Redox regulation of endothelial cell fate. Cell Mol Life Sci 71: 3219-3239, 2014.
20. Fandy TE, Jiemjit A, Thakar M, Rhoden P, Suarez L and Gore SD: Decitabine induces delayed reactive oxygen species (ROS) accumulation in leukemia cells and induces the expression of ROS generating enzymes. Clin Cancer Res 20: 1249-1258, 2014.
21. Borradaile NM, Han X, Harp JD, Gale SE, Ory DS and Schaffer JE: Disruption of endoplasmic reticulum structure and integrity in lipotoxic cell death. J Lipid Res 47: 2726-2737, 2006.
22. Xu MJ, Song P, Shirwany N, Liang B, Xing J, Viollet B, Wang X, Zhu Y and Zou MH: Impaired expression of uncoupling protein 2 causes defective postischemic angiogenesis in mice deficient in AMP-activated protein kinase alpha subunits. Arterioscler Thromb Vasc Biol 31: 1757-1765, 2011.
23. Jansen F, Yang X, Hoelscher M, Cattelan A, Schmitz T, Proebsting S, Wenzel D, Vosen S, Franklin BS, Fleischmann BK, *et al*: Endothelial microparticle-mediated transfer of MicroRNA-126 promotes vascular endothelial cell repair via SPRED1 and is abrogated in glucose-damaged endothelial microparticles. Circulation 128: 2026-2038, 2013.
24. Yan Y and Finkel T: Autophagy as a regulator of cardiovascular redox homeostasis. Free Radic Biol Med 109: 108-113, 2017.

25. Li L, Tan J, Miao Y, Lei P and Zhang Q: ROS and autophagy: Interactions and molecular regulatory mechanisms. Cell Mol Neurobiol 35: 615-621, 2015.
26. Filomeni G, De Zio D and Cecconi F: Oxidative stress and autophagy: The clash between damage and metabolic needs. Cell Death Differ 22: 377-388, 2015.
27. Papandreou I, Lim AL, Laderoute K and Denko NC: Hypoxia signals autophagy in tumor cells via AMPK activity, independent of HIF-1, BNIP3, and BNIP3L. Cell Death Differ 15: 1572-1581, 2008.
28. Tang D, Kang R, Cheh CW, Livesey KM, Liang X, Schapiro NE, Benschop R, Sparvero LJ, Amoscato AA, Tracey KJ, *et al*: HMGB1 release and redox regulates autophagy and apoptosis in cancer cells. Oncogene 29: 5299, 2010.
29. Tang D, Kang R, Livesey KM, Cheh CW, Farkas A, Loughran P, Hoppe G, Bianchi ME, Tracey KJ, Zeh HJ III and Lotze MT: Endogenous HMGB1 regulates autophagy. J Cell Biol 190: 881-892, 2010.
30. Guzy RD, Hoyos B, Robin E, Chen H, Liu L, Mansfield KD, Simon MC, Hammerling U and Schumacker PT: Mitochondrial complex III is required for hypoxia-induced ROS production and cellular oxygen sensing. Cell Metab 1: 401-408, 2005.
31. Bellot G, Garcia-Medina R, Gounon P, Chiche J, Roux D, Pouysségur J and Mazure NM: Hypoxia-induced autophagy is mediated through hypoxia-inducible factor induction of BNIP3 and BNIP3L via their BH3 domains. Mol Cell Biol 6: 2570-2581, 2009.
32. Lob H, Rosenkranz AC, Breitenbach T, Berkels R, Drummond G and Roesen R: Antioxidant and nitric oxide-sparing actions of dihydropyridines and ACE inhibitors differ in human endothelial cells. Pharmacology 76: 8-18, 2006.
33. Zhang C, Lan T, Hou J, Li J, Fang R, Yang Z, Zhang M, Liu J and Liu B: NOX4 promotes non-small cell lung cancer cell proliferation and metastasis through positive feedback regulation of PI3K/Akt signaling. Oncotarget 5: 4392-4405, 2014.